

Investigation of degradation and recovery characteristics of NBTI in 28-nm high-*k* metal gate process

Wei-Tai Gong(巩伟泰), Yan Li(李闫), Ya-Bin Sun(孙亚宾), Yan-Ling Shi(石艳玲), and Xiao-Jin Li(李小进)
Citation: Chin. Phys. B, 2023, 32 (**12**): 128502. DOI: 10.1088/1674-1056/ace034
Journal homepage: http://cpb.iphy.ac.cn; http://iopscience.iop.org/cpb

What follows is a list of articles you may be interested in

Dynamic modeling of total ionizing dose-induced threshold voltage shifts in MOS devices

Guangbao Lu(陆广宝), Jun Liu(刘俊), Chuanguo Zhang(张传国), Yang Gao(高扬), and Yonggang Li(李永钢)
Chin. Phys. B, 2023, 32 (**1**): 018506. DOI: 10.1088/1674-1056/ac9fc4

Enhanced radiation-induced narrow channel effects in 0.13-μm PDSOI nMOSFETs with shallow trench isolation

Meng-Ying Zhang(张梦映), Zhi-Yuan Hu(胡志远), Da-Wei Bi(毕大炜), Li-Hua Dai(戴丽华), Zheng-Xuan Zhang(张正选)
Chin. Phys. B, 2018, 27 (**2**): 028501. DOI: 10.1088/1674-1056/27/2/028501

Detailed study of NBTI characterization in 40-nm CMOS process using comprehensive models

Yan Zeng(曾严), Xiao-Jin Li(李小进), Jian Qing(卿健), Ya-Bin Sun(孙亚宾), Yan-Ling Shi(石艳玲), Ao Guo(郭奥), Shao-Jian Hu(胡少坚)
Chin. Phys. B, 2017, 26 (**10**): 108503. DOI: 10.1088/1674-1056/26/10/108503

Influence of white light illumination on the performance of a-IGZO thin film transistor under positive gate-bias stress

Tang Lan-Feng (汤兰凤), Yu Guang (于广), Lu Hai (陆海), Wu Chen-Fei (武辰飞), Qian Hui-Min (钱慧敏), Zhou Dong (周东), Zhang Rong (张荣), Zheng You-Dou (郑有炓), Huang Xiao-Ming (黄晓明)
Chin. Phys. B, 2015, 24 (**8**): 088504. DOI: 10.1088/1674-1056/24/8/088504

Positive gate-bias temperature instability of ZnO thin-film transistor

Liu Yu-Rong (刘玉荣), Su Jing (苏晶), Lai Pei-Tao (黎沛涛), Yao Ruo-He (姚若河)
Chin. Phys. B, 2014, 23 (**6**): 068501. DOI: 10.1088/1674-1056/23/6/068501

Investigation of degradation and recovery characteristics of NBTI in 28-nm high-*k* metal gate process

Wei-Tai Gong(巩伟泰), Yan Li(李闫), Ya-Bin Sun(孙亚宾), Yan-Ling Shi(石艳玲), and Xiao-Jin Li(李小进)†

Shanghai Key Laboratory of Multidimensional Information Processing and the Department of Electrical Engineering, East China Normal University, Shanghai 200241, *China*

(Received 16 April 2023; revised manuscript received 19 June 2023; accepted manuscript online 21 June 2023)

Degradation induced by the negative bias temperature instability (NBTI) can be attributed to three mutually uncoupled physical mechanisms, i.e., the generation of interface traps ($\Delta V_{\rm IT}$), hole trapping in pre-existing gate oxide defects ($\Delta V_{\rm HT}$), and the generation of gate oxide defects ($\Delta V_{\rm OT}$). In this work, the characteristic of NBTI for p-type MOSFET fabricated by using a 28-nm high-*k* metal gate (HKMG) process is thoroughly studied. The experimental results show that the degradation is enhanced at a larger stress bias and higher temperature. The effects of the three underlying subcomponents are evaluated by using the comprehensive models. It is found that the generation of interface traps dominates the NBTI degradation during long-time NBTI stress. Moreover, the NBTI parameters of the power-law time exponent and temperature activation energy as well as the gate oxide field acceleration are extracted. The dependence of operating lifetime on stress bias and temperature is also discussed. It is observed that NBTI lifetime significantly decreases as the stress increases. Furthermore, the decrease of charges related to interface traps and hole detrapping in pre-existing gate oxide defects are used to explain the recovery mechanism after stress.

Keywords: negative bias temperature instability (NBTI), high-*k* metal gate (HKMG), threshold voltage shift, interface trap, gate oxide defect

PACS: 85.30.De, 73.40.Qv, 72.20.Jv **DOI:** 10.1088/1674-1056/ace034

1. Introduction

With transistors scaling down, high-*k* metal gate (HKMG) has become a significant technology for 28-nm advanced process.[1] However, negative bias temperature instability (NBTI) has become a very important research subject in HKMG devices.[2–5] In a real circuit, it could seriously degrade some important parameters, such as the mobility, the threshold voltage ($V_{\rm T}$), the saturation drain current ($I_{\rm DSAT}$), and transconductance ($g_{\rm m}$).[6–13] As a result, the lifetime of stressed device and the reliability of circuit deteriorate over time.

The physical mechanism of NBTI has been extensively investigated through comprehensive models established by several research groups. Commonly consistent results are achieved from the fact that three subcomponents contribute to the degradation of NBTI, i.e., generated interface traps ($\Delta N_{\rm IT}$), hole traps in pre-existing gate oxide defects ($\Delta N_{\rm HT}$), and generated gate oxide traps ($\Delta N_{\rm OT}$).[14–16] Note that they were treated as being uncoupled with each other. The generation of interface traps ($\Delta N_{\rm IT}$) followed a power-law dependence on time in long-time NBTI stress and could be well described by using the double interface reaction–diffusion (RD) model.[17] For an HKMG device, the interface trap generation ($\Delta N_{\rm IT}$) was ascribed to the breaking of Si–H bonds at the Si/interlayer (IL) interface and the diffusion of hydrogen molecular (H_2) generated by the reaction of hydrogen atoms (H) with *X*–H bonds at the IL/high-*K* interface, with the *X* representing oxygen or nitrogen-related gate oxide defect. The hole trapping in pre-existing gate oxide defects ($\Delta N_{\rm HT}$) was extremely sensitive to the gate nitriding process since the nitrogen could diffuse into gate oxide layer and thus creating original defects.[18–20] Note that it usually reached to a saturated state within a few seconds. The generation of gate oxide defects ($\Delta N_{\rm OT}$) represents the contribution of hole trapping to overall degradation that occurs owing to fresh traps created in thicker gate oxide under higher stress. For most of HKMG devices with thinner oxide dielectric, $\Delta N_{\rm OT}$ may be negligible. At the beginning of recovery, a fraction of electrons captured which are associated with interface traps[21] and holes detrapped in pre-existing gate oxide defects recover rapidly. After that, the long-time recovery process dominated the passivation of interface traps, induced by the back diffusion of H_2 molecules.[22,23] However, a fraction of H_2 molecules could not be recovered owing to being locked within the traps during stress.

In this work, we study the characteristics of NBTI degradation and recovery for 28-nm HKMG p-MOSFETs by using the experimental data and the comprehensive models. The NBTI parameters including power-law time exponent (n), temperature activation energy ($E_{\rm A}$), and oxide field acceleration factor ($I_{\rm E}$) are extracted. The influence of long-time NBTI stress biases ($V_{\rm G-STR}$) and temperatures (T) on device operating lifetime are accurately evaluated. Furthermore, the long-time recovery behaviors of devices are also analyzed by using comprehensive models.

†Corresponding author. E-mail: xjli@ee.ecnu.edu.cn

© 2023 Chinese Physical Society and IOP Publishing Ltd

2. Device and experiment

The p-MOSFETs used in this work were fabricated by the 28-nm HKMG process technology. The device had an equivalent oxide thickness (EOT) of 1.75 nm. In order to evaluate the influence of NBTI degradation, the values of threshold voltage (V_T) were obtained under different values of stress V_{G-STR} (1.4 V, 1.5 V, and 1.6 V) and different values of temperature T (80 °C, 100 °C, and 125 °C) at fixed stress time t_{STR} (3000 s). The fresh threshold voltage (V_{T0}) of device has been extracted through the constant current method. The drain to source voltage of $V_D = 0.05$ V was held to keep the device in linear region, with both source and substrate grounded. As the gate to source voltage (V_G) increased until the drain current reaches 0.1 μA×W/L, V_T could be obtained by V_G. Figure 1 shows the NBTI measurement setup of HKMG device through using the measure–stress–measure (MSM) method. Firstly, the transfer characteristic of fresh device was measured to extract the V_T. Then, the stress was applied, and after that the V_T was measured periodically during the measurement. In this way, the dependence of threshold voltage shift (ΔV_T) on the t_{STR} variation could be obtained.

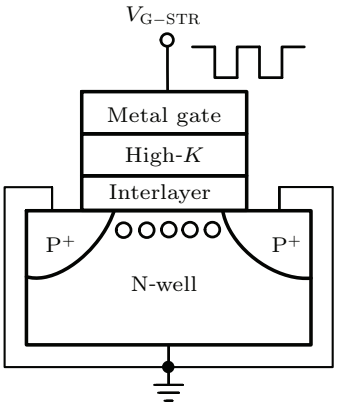


Fig. 1. Schematic diagram of measurement setup to characterize NBTI stress.

3. Results and discussion

3.1. Degradation characteristics

As mentioned above, the threshold voltage shift induced by the NBTI in HKMG device is composed of three parts caused by uncoupled physical mechanisms, i.e., ΔN_{IT}, ΔN_{HT}, and ΔN_{OT},[16] and can be written as

$$\Delta V_T = \frac{q}{C_{OX}} \times (\Delta N_{IT} + \Delta N_{HT} + \Delta N_{OT}), \tag{1}$$

where q is the electronic charge, and C_{OX} is the gate oxide capacitance. The degradation of the threshold voltage induced by the interface trap (ΔN_{IT}) can be described by the double interface reaction diffusion model[24,25] as shown in Fig. 2(a). The Si–H bonds are assumed to be located at the Si/IL interface, which is named the first interface of the HKMG device. The X–H bonds are located at the second interface, which is defined at some distance away from the first interface. The X represents oxygen or nitrogen-related defect. When the NBTI stress is applied, weak covalent Si–H bonds are easily broken by the collision under the stress, leading to the formation of unbonded Si or interfacial traps at the Si/IL interface. Owing to the concentration gradient, the H atoms released from the broken Si–H bond begin to diffuse towards the gate and can form H_2 molecules by reacting with the X–H bond at the IL/high-K interface. The ΔN_{IT} has a power-law dependence on time for long-time stress[22,26] and can be written as

$$\Delta N_{IT} = A E_{OX} \, e^{\Gamma_{IT} E_{OX}} \, e^{-E_{AIT}/kT} t_{STR}^{n}, \tag{2}$$

where E_{OX} is the gate oxide field, E_{AIT} is the temperature activation, A is the fitting parameter, kT is the thermal energy, n is the power-law time exponent, and Γ_{IT} is the gate oxide field acceleration, which are all process-dependent and need modelling for the HKMG process. Moreover, the degradation of fresh threshold voltage is included in the degradation process by the calculation of E_{OX}. Using the iterative method, more accurate result can be obtained from the following equation:

$$E_{OX} = (V_{G-STR} - V_{T0} - \Delta V_T)/\text{EOT}. \tag{3}$$

The temperature activation for interface trap (E_{AIT}) consists of molecular H_2 diffusion (E_{ADH2}), forward breaking (E_{AKF}) and reverse passivation (E_{AKR}) of the Si–H bond.[27] Hence, it is written as

$$E_{AIT} = \frac{2}{3}(E_{AKF} - E_{AKR}) + \frac{E_{ADH2}}{6}. \tag{4}$$

E_{AKR} of 0.2 eV and E_{ADH2} of 0.58 eV are fixed in different HKMG devices, and E_{AKF} is the only process-dependent factor and needs modelling according to the various experimental data.

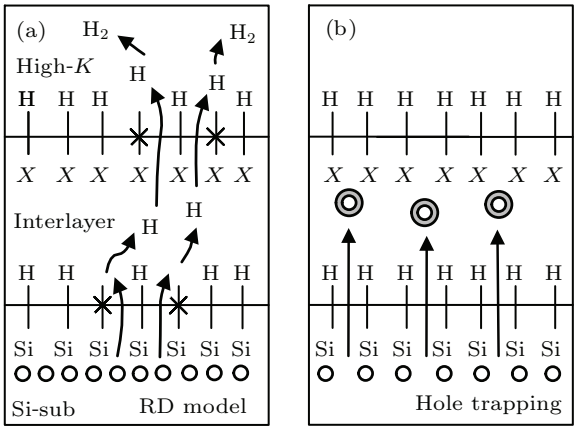


Fig. 2. Schematic diagram of (a) double interface reaction diffusion model and (b) hole trapping in pre-existing gate oxide defects during NBTI degradation.

The hole trapping model and detrapping model are another explanation for the NBTI.[25] As is well known, a great number of defects can be generated inside gate insulator in the manufacturing process. When gate stress bias is applied, the holes are trapped by the pre-existing gate oxide defects, which

causes these defects to be positively charged, thereby leading the threshold voltage to shift as shown in Fig. 2(b). The studies have confirmed that ΔN_{HT} is saturated and reaches a constant value for long-time stress,[22] and can be expressed as

$$\Delta N_{HT} = BE_{OX} e^{\Gamma_{HT} E_{OX}} e^{-E_{AHT}/kT}, \quad (5)$$

where the parameter B and oxide field acceleration factor Γ_{HT} are related to the fabrication process. The temperature activation energy for ΔN_{HT} (E_{AHT}) is fixed at a value of 0.052 eV for different processes. According to the generation mechanism of bulk gate oxide defects, the time evolution of ΔN_{OT} is represented by a stretched exponential form,[22] and it is expressed as

$$\Delta N_{OT} = C\left(1 - e^{(-t/w)^{\beta_{OT}}}\right), \quad (6)$$

where the parameter $\beta_{OT} = 0.33$ is kept unchanged for various processes, and C is related to the fabrication process. It is important to remark that trap generation in gate insulator is negligible for HKMG devices owing to thinner EOT at lower V_{G-STR}.[16,28,29] In this work, ΔN_{OT} is not considered for this low voltage core logic device.

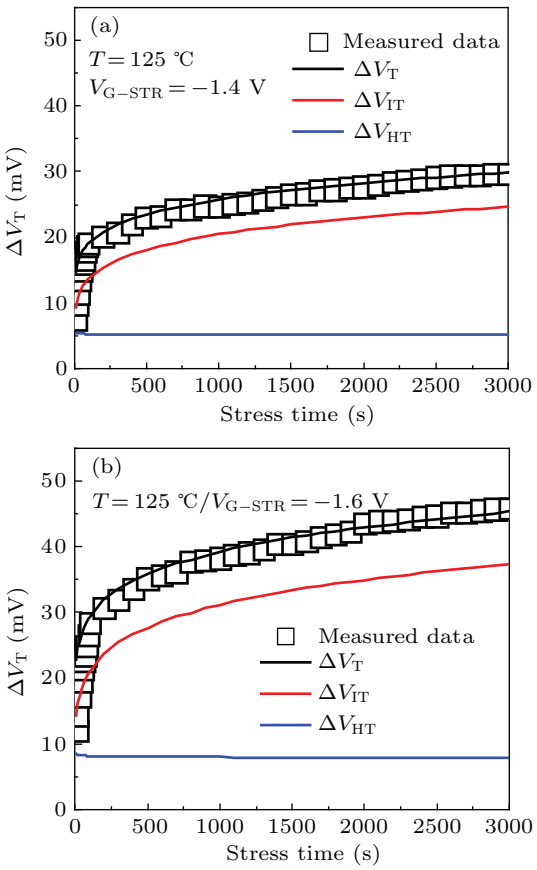


Fig. 3. Curves of measured (symbols) and model-calculated ΔV_T, ΔV_{IT}, ΔV_{HT} subcomponents (lines) at 125 °C, V_{G-STR} of −1.4 V (a) and −1.6 V (b), respectively.

Figure 3 shows the time evolutions of measured and calculated ΔV_T as well as its subcomponents for HKMG devices at V_{G-STR} = 1.4 V and 1.6 V, respectively. Note that the ΔN_{OT} is negligible and the overall degradation only considers the ΔN_{IT} and ΔN_{HT} subcomponents. It can be seen that the experimental data are consistent with the calculations from the model for the NBTI degradation. The time evolution of ΔV_T increases rapidly at the onset of stress and shows the power-law dependence for long stress time. It can be observed that the ΔN_{IT} dominates the majority of ΔV_T during the NBTI stress, whereas the ΔN_{HT} is saturated in a few seconds and then keeps constant. The reason is that the contribution from the generated interface traps continuously increases for long stress time, however, the hole trapping in pre-existing bulk gate oxide defects is a fast process. The ΔN_{IT} also shows a power-law time dependence and increases as the V_{G-STR} increases. Given $t_{STR} = 3 \times 10^3$ s, when the V_{G-STR} reaches 1.4 V, the contribution from ΔN_{IT} is 24.67 mV compared with 37.38 mV as the V_{G-STR} becomes 1.6 V. However, the contribution from the ΔN_{HT} changes slightly as the V_{G-STR} increases, giving 5.2 mV@V_{G-STR} = 1.4 V, 7.9 mV@V_{G-STR} = 1.6 V, respectively. Figure 4 shows the time evolutions of measured and calculated ΔV_T at different values of V_{G-STR} and temperature, demonstrating that the experimental data can be accurately predicted by the models.

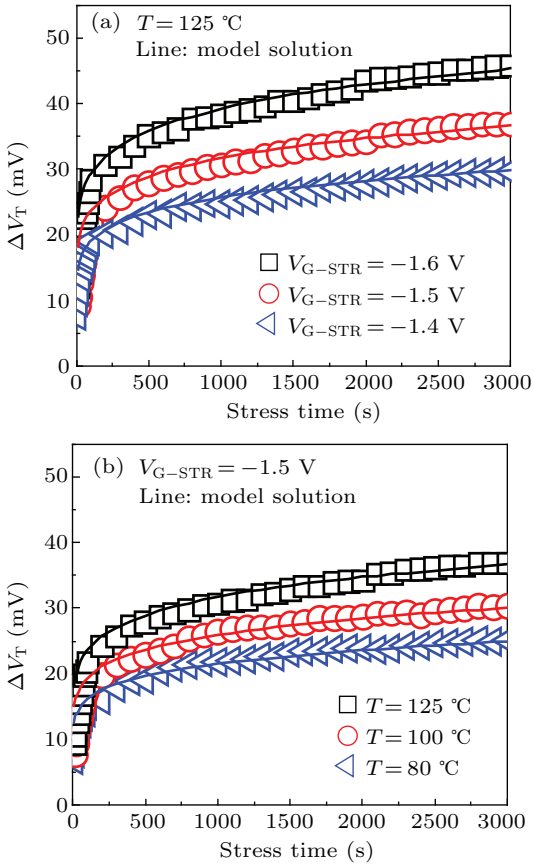


Fig. 4. Curves of measured (symbols), model-calculated ΔV_T (lines) for different values of V_{G-STR} (a) and temperature (b), with identical model parameters used. The extracted parameters: $(q/C_{OX}) \times A = 4.2 \times 10^{-9}$ (1/cm·s$^{0.18}$), Γ_{IT} ($= \Gamma_{HT}$) = 0.24 (cm/MV), E_{AKF} = 0.205 eV, n = 0.18, $(q/C_{ox}) \times B = 9.32 \times 10^{-10}$ (1/cm), C = 0 (ΔV_{OT} is negligible for HKMG devices at low stress bias).

Furthermore, the dependence of relative contributions from underlying $\Delta N_{\rm IT}$ and $\Delta N_{\rm HT}$ on temperature and $t_{\rm STR}$ are analyzed. Figures 5(a) and 5(b) show the evolution of relative contributions from $\Delta N_{\rm IT}$ and $\Delta N_{\rm HT}$ to the accumulated degradation *versus* T at fixed $V_{\rm G-STR} = 1.5$ V but different $t_{\rm STR}$, respectively. It can be seen that $\Delta N_{\rm IT}$ has a strong dependence on $t_{\rm STR}$, longer $t_{\rm STR}$ larger $\Delta V_{\rm IT}$. The relative contribution of $\Delta N_{\rm IT}$ can reach up to 90% for the longest stress time even at room temperature, as shown in Fig. 5(a). $\Delta N_{\rm IT}$ contributes the most degradation and the impact of $\Delta N_{\rm HT}$ weakens over longer $t_{\rm STR}$. On the contrary, when $t_{\rm STR}$ is short enough, the relative contribution from $\Delta N_{\rm HT}$ is higher because the hole trapping in pre-existing gate insulator can be saturated in few seconds, as shown in Fig. 5(b).

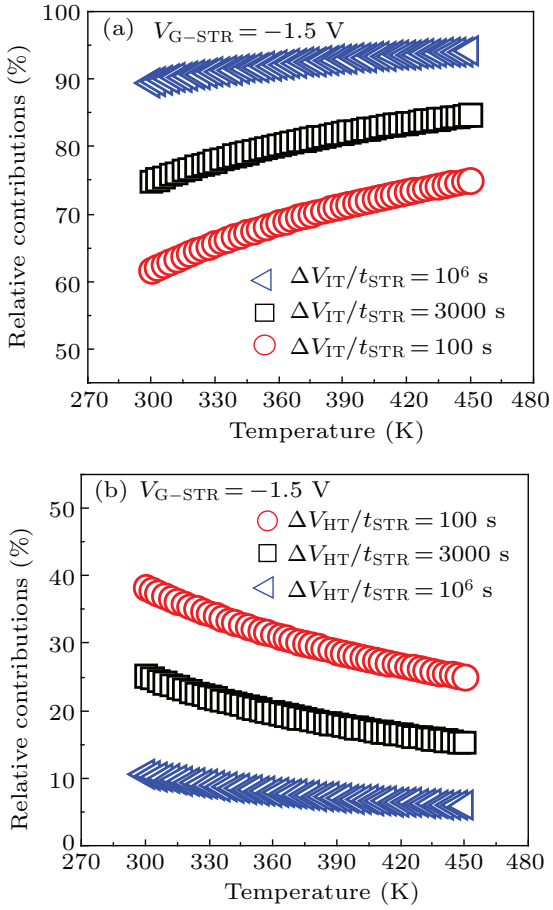


Fig. 5. Relative contributions *versus* temperature for different values of $\Delta V_{\rm IT}/t_{\rm STR}$ (a) and $\Delta V_{\rm HT}/t_{\rm STR}$ (b).

The dependence of NBTI degradation on channel length in HKMG p-MOSFETs is also studied. Taking the channel length into account, equation (1) can be revised as follows:

$$\Delta V_{\rm T} = \frac{q}{C_{\rm OX}} \times L^m \times (\Delta N_{\rm IT} + \Delta N_{\rm HT} + \Delta N_{\rm OT}), \tag{7}$$

where L is the channel length, and m is the fitting parameter. Figure 6 shows the time evolution of $\Delta V_{\rm T}$ under the fixed $V_{\rm G-STR}$ and T, for the different channel lengths. The shorter the length L, the less the NBTI degradation is; as the L shrinks from 1000 nm to 30 nm, the NBTI degradation decreases from 36.9 mV to 12.7 mV at $t_{\rm STR} = 3000$ s, correspondingly. The root cause is that in the post-gate high-temperature process steps in oxygen atmosphere, the oxygen diffuses into the high-k layer at the corners of active-gate overlapping region and annihilates the positively charged oxygen vacancies.[6,30] This process reduces the average number of oxygen vacancies per gate area in narrow and short device, and thus the NBTI degradation is also alleviated.

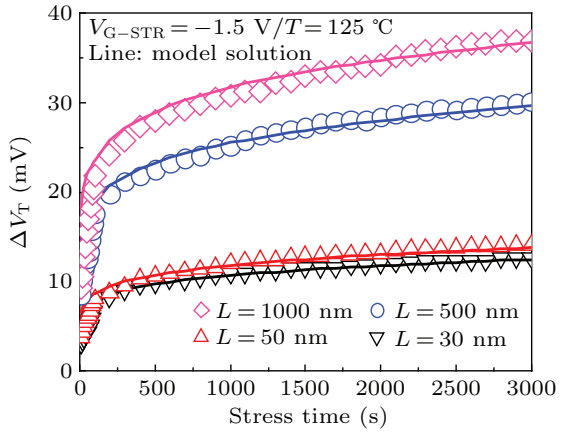


Fig. 6. Time evolutions of $\Delta V_{\rm T}$ for different channel lengths at fixed $V_{\rm G-STR}$ of -1.5 V at $T = 125$ °C, and the extracted parameters: $m = 0.37$ for different values of L.

From a practical point of view, it is essential to estimate the working lifetime of the device. The working lifetime of HKMG device is defined as the length of working time before its threshold voltage shift exceeds 50 mV.[31] Figure 7 illustrates the variations of operating lifetime with $V_{\rm G-STR}$ at different values of T, calculated from the model together with the extracted parameters. The model prediction shows that the higher $V_{\rm G-STR}$ and T lead to the higher NBTI degradation. Consequently, the NBTI lifetime is significantly reduced as well.

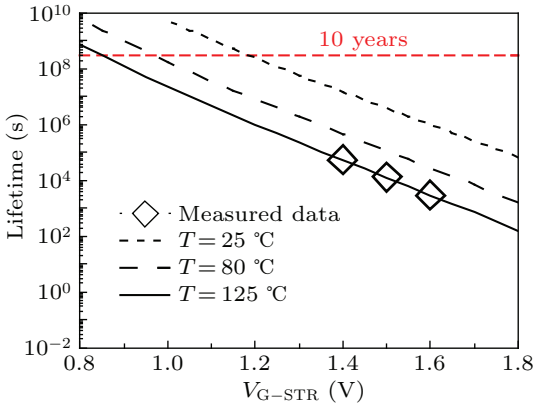


Fig. 7. Variations of NBTI lifetime with $V_{\rm G-STR}$ for HKMG p-MOSFETs at different temperatures.

3.2. Discussion on NBTI parameters

3.2.1. Power-law time exponent

The $\Delta V_{\rm T}$ versus time shows a power-law dependence under long-time stress. The working lifetime can be significantly

reduced as the time exponent (n) increases, hence it is essential to extract the time exponent n for HKMG device. It is observed that the time evolution of $\Delta V_{\rm T}$ shows a parallel relation to each other in log–log scale diagram with different $V_{\rm G-STR}$. Then the value of n can be extracted in the linear regression of measured $\Delta V_{\rm T}$ versus time evolution in a fixed range of $t_{\rm STR} = 1000$ s to 3000 s. Figure 8 shows the power law time exponent (n) as a function of various $V_{\rm G-STR}$ in HKMG p-MOSFET. It is crucial to find that the degradation shows a similar power-law time dependence with n of 0.18 for different values of $V_{\rm G-STR}$. Moreover, it indicates that $\Delta N_{\rm IT}$ dominates the degradation under long-time NBTI stress. Note that the measured data are from the HKMG device with thinner EOT under lower stress conditions, hence $\Delta N_{\rm OT}$ is neglected.

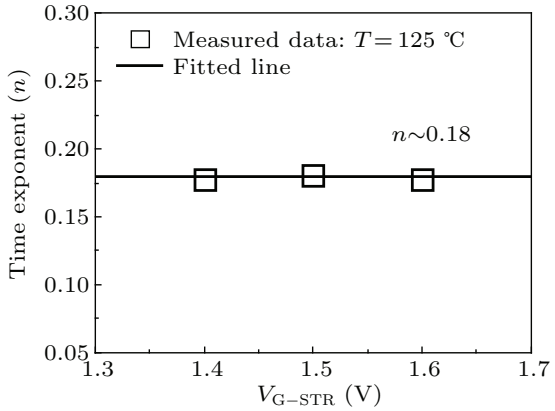


Fig. 8. Extracted power-law time exponent n versus $V_{\rm G-STR}$, measured and fitted at $T = 125$ °C.

3.2.2. Temperature-activation energy

Figure 9 shows the measured $\Delta V_{\rm T}$ as a function of T at a fixed $t_{\rm STR}$ of 2000 s. It is clear that $\Delta V_{\rm T}$ presents the linear dependence of T on a semi-log scale, and hence the temperature-activation energy ($E_{\rm A}$) which is close to 0.096 eV is extracted from Fig. 9. It is important to remark that $\Delta N_{\rm IT}$ contributes most of degradation, and the $E_{\rm AHT}$ (0.052 eV) of $\Delta N_{\rm HT}$[16] is lower than that of $\Delta N_{\rm IT}$. On the one hand, the time evolution of $\Delta N_{\rm IT}$ is mainly determined by the diffusion of

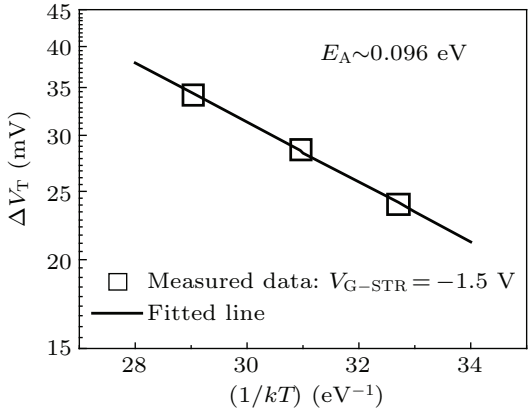


Fig. 9. Measured $\Delta V_{\rm T}$ as a function of temperature at fixed $t_{\rm STR}$ of 2000 s.

molecular H_2 under long-time stress. The $E_{\rm AKF}$ for forward breaking is close to the $E_{\rm AKR}$ for reverse passivation of the Si–H bond. It can be seen that $E_{\rm AIT}$ of $\Delta N_{\rm IT}$ is similar to that of $E_{\rm ADH2}/6$ (about 0.1 eV), whereas $E_{\rm ADH2}$ is temperature-activation of H_2 molecular diffusion. As a result, the extracted $E_{\rm A}$ (0.096 eV) is slightly lower than 0.1 eV when the contribution of $\Delta N_{\rm HT}$ is considered.

3.2.3. Field acceleration factor

As discussed above, the hole trapping in inverse layer leads Si–H bonds to break and defects to generate at the Si/IL interface, resulting in an increase in $\Delta N_{\rm IT}$. Similarly, the hole trapping in pre-existing gate oxide defects makes $\Delta N_{\rm HT}$ accumulate. $\Delta N_{\rm IT}$ and $\Delta N_{\rm HT}$ have the same $E_{\rm OX}$ dependence ($\Gamma_{\rm IT} = \Gamma_{\rm HT}$). Figure 10 shows the measured $\Delta V_{\rm T}$ as a function of $E_{\rm OX}$ at given stress time $t_{\rm STR} = 3000$ s. The oxide field acceleration ($\Gamma_{\rm E}$) is also extracted from the slope of fitting line, giving a value of 0.231 cm/MV.

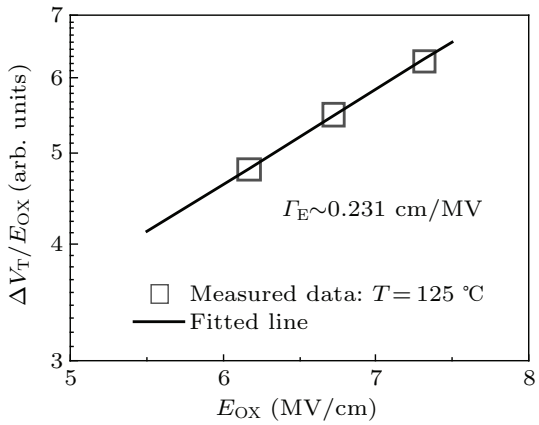


Fig. 10. Measured and fitted $\Delta V_{\rm T}$ as a function of stress $E_{\rm OX}$ at fixed $t_{\rm STR}$ and $T = 125$ °C.

3.3. Recovery characteristics

Once the gate stress is removed, the energy of a fraction of $\Delta N_{\rm IT}$ may move below the Fermi level of substrate and recover rapidly by capturing electrons within a few seconds. Then, the remaining part of $\Delta N_{\rm IT}$ recovers owing to the back diffusion of H_2 and H, which leads to the passivation of the broken bonds at the interface. It is important to remark that this is a slow process. The double interface reaction diffusion model can predict the physics process of slow recovery. At the beginning, the H_2 molecule reacts with the broken X-bonds at the IL/high-K interface and generates H atoms. After that, the H atoms diffuse towards the Si/IL interface and passivate the broken Si bonds, resulting in the recovery of $\Delta N_{\rm IT}$. Of course, the probability of H_2 finding the interface defects decreases as the recovery time lapses, which can be expressed as the decrease of diffusion coefficient of H_2 with time. Note that a

fraction of H species may be locked by the defects, resulting in a permanent degradation that cannot be recovered.[32]

Furthermore, the recovery of pre-existing and generated gate insulator defects is a fast process that is depicted by hole detrapping when the stress voltage is withdrawn. Because the trap generation in gate insulator is negligible for thinner EOT device and lower $V_{\mathrm{G-STR}}$, the recovery due to ΔN_{OT} is also excluded during NBTI recovery.

As a result, the overall recovery of threshold voltage shift consists of fast electron capturing (ΔV_{IT1}), slow recovery of interface traps (ΔV_{IT2}), and fast hole detrapping of pre-existing gate insulator traps (ΔV_{HT}). The total recovery can be expressed as

$$\Delta V_{\mathrm{T}} = \Delta V_{\mathrm{IT1}} + \Delta V_{\mathrm{IT2}} + \Delta V_{\mathrm{HT}}. \tag{8}$$

In order to assess the contribution of ΔV_{IT2} to overall recovery, an analytical model extrapolated from double interface reaction diffusion theory is used to calculate ΔV_{IT2} that is written as[32]

$$\Delta V_{\mathrm{IT2}} = \Delta V_{\mathrm{IT0}}\,(1-F_{\mathrm{FAST}})\,\alpha + \Delta V_{\mathrm{IT0}}\,(1-F_{\mathrm{FAST}})\,(1-\alpha) \times \left(1-\sqrt{\frac{\xi t_{\mathrm{REC}}}{t_{\mathrm{STR}}+t_{\mathrm{REC}}}}\right), \tag{9}$$

where F_{FAST} denotes the fast recovery component of ΔN_{IT}, α is the scaling factor of non-recoverable component due to H species locked in the trap, and ξ represents the decrease of H_2 diffusion with time going by. Note that the parameter ξ can be approximately treated as a constant when $t_{\mathrm{REC}} < t_{\mathrm{STR}}$.[33] ΔV_{IT0} is the total degradation before the recovery starts, and can be obtained by using the NBTI stress model. The empirical expression describing the fast recovery contribution of ΔV_{IT1} and ΔV_{HT} are, respectively, proposed[32] as follows:

$$\Delta V_{\mathrm{IT1}} = \Delta V_{\mathrm{IT0}} \cdot F_{\mathrm{FAST}} \cdot \exp\left[-\left(\frac{t_{\mathrm{REC}}}{\tau_{\mathrm{EC}}}\right)^{\beta_{\mathrm{EC}}}\right], \tag{10}$$

$$\Delta V_{\mathrm{HT}} = \Delta V_{\mathrm{HT0}} \cdot \exp\left[-\left(\frac{t_{\mathrm{REC}}}{\tau_{\mathrm{REC}}}\right)^{\beta_{\mathrm{REC}}}\right], \tag{11}$$

where τ_{EC} is the electron capture time constant, and τ_{REC} is the hole detrapping time constant. The stretched-exponential form is used to describe the time constant dispersion with the parameters β_{EC} and β_{REC}, and ΔV_{HT0} is also obtained from the NBTI stress model discussed above.

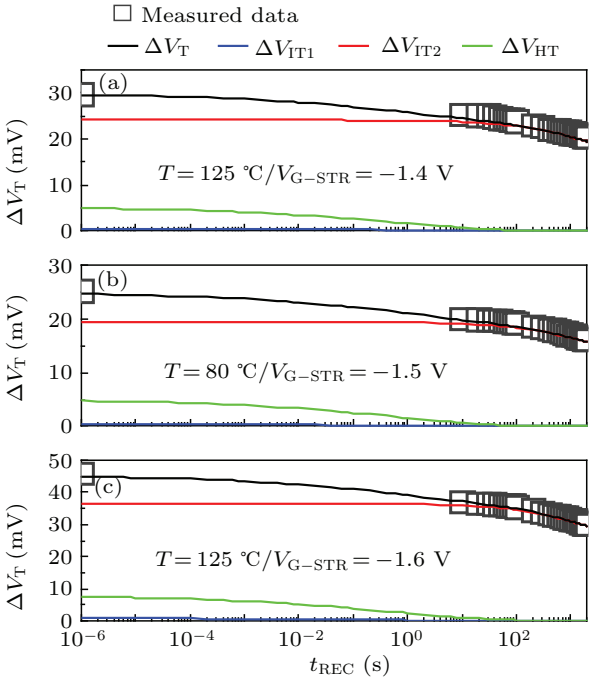


Fig. 11. Measured and calculated ΔV_{T} as well as its underlying subcomponents recovery (ΔV_{IT1}, ΔV_{IT2}, and ΔV_{HT}) as a function of recovery time after different values of NBTI $V_{\mathrm{G-STR}}$ and temperature during $V_{\mathrm{G-REC}} = 0$ V. And the extracted parameters: $(1-F_{\mathrm{FAST}})(1-\alpha)\xi^{1/2} = 0.3$, $F_{\mathrm{FAST}} = 0.02$, $\tau_{\mathrm{EC}} = 0.82$, $\beta_{\mathrm{EC}} = 0.36$, $\tau_{\mathrm{REC}} = 0.5$, and $\beta_{\mathrm{REC}} = 0.23$.

Figure 11 plots the time evolution of measured and calculated ΔV_{T} recovery under stress for different values of $V_{\mathrm{G-STR}}$ and T, in which the underlying three subcomponents calculated by the models are also shown. It is clear that the process of electron capturing and hole detrapping recover fast. The long-time recovery occurs based on the trap passivation induced by the slow back diffusion of H_2.

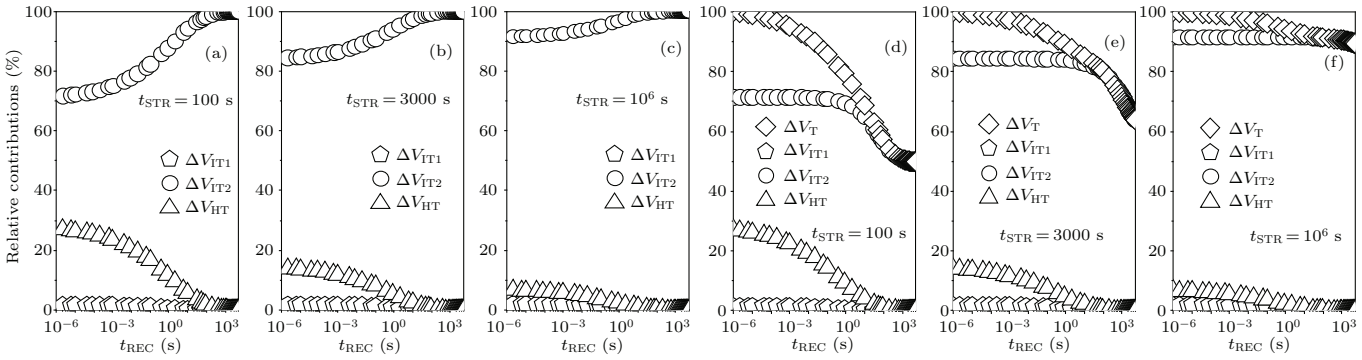


Fig. 12. Time kinetics of relative contribution from ΔV_{IT1}, ΔV_{IT2}, and ΔV_{HT} to the remaining overall degradation at $t_{\mathrm{STR}} = 100$ s (a), 300 s (b), and 10^6 s (c), and the time kinetics of relative contribution from ΔV_{IT1}, ΔV_{IT2}, ΔV_{HT}, and ΔV_{T} to the initial degradation before recovery at $t_{\mathrm{STR}} = 100$ s (d), 300 s (e), and 10^6 s (f), with $V_{\mathrm{G-STR}} = -1.5$ V, $V_{\mathrm{G-REC}} = 0$ V, and $T = 125$ °C.

Figure 12 shows the time evolution of the calculated $\Delta V_{\rm T}$ and underlying $\Delta V_{\rm IT1}$, $\Delta V_{\rm IT2}$, and $\Delta V_{\rm HT}$ by using the comprehensive model and extracted parameters. It is observed that as the stress time decreases, the contribution of $\Delta V_{\rm HT}$ increases. Consequently, the overall recovery turns out to be faster. For the stress times such as 100 s, 3000 s, and 10^6 s, shown in Figs. 12(a)–12(c), the recovery times for $\Delta V_{\rm IT2}$ which contributes to 99% of the remaining degradation are 200 s, 60 s, and 20 s, respectively, demonstrating that $\Delta V_{\rm IT2}$ dominates the slow process through H_2 back diffusion during long-time recovery.

Figure 13 shows the time evolution of the measured and the calculated $\Delta V_{\rm T}$, and its underlying subcomponents at different values of NBTI $V_{\rm G-STR}$ and T for the p-MOSFETs. The comprehensive models fit the measured data well. It is noteworthy that about 34% of overall degradation for these devices recovers at 2000 s. For the stress voltage of 1.4 V, 1.5 V, and 1.6 V, the recovery at 125 °C after 2000 s reaches to 31.4%, 34.9%, and 34.7%, respectively. For $V_{\rm G-STR} = 1.5$ V and $T = 80$ °C, the recovery also arrives at 35.8%.

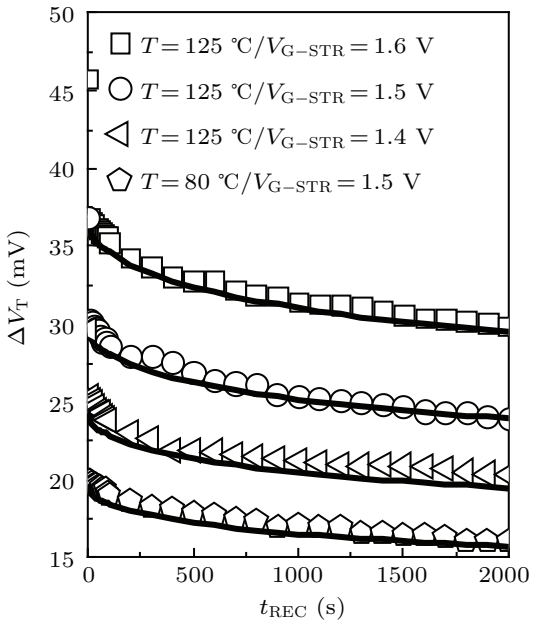


Fig. 13. Time evolution of measured and calculated $\Delta V_{\rm T}$ recovery for different values of NBTI $V_{\rm G-STR}$ and temperature.

4. Conclusions

In summary, the NBTI characteristics of degradation and recovery are studied for 28-nm HKMG p-MOSFETs by using comprehensive models. It is shown that the extracted parameters reflect the long-time NBTI characteristics well. The contribution of the independent underlying subcomponents $\Delta V_{\rm IT}$ and $\Delta V_{\rm HT}$ to overall degradation is calculated, and the results indicate that the $\Delta V_{\rm IT}$ dominated the NBTI degradation during stress experiments. The reason behind this behavior is that the $\Delta V_{\rm IT}$ shows power-law time dependence of $n = 0.18$ at long-time degradation, while $\Delta V_{\rm HT}$ is saturated in a few seconds. Meanwhile, NBTI parameters including the power-law time exponent of 0.18, temperature activation energy of 0.096 eV, and gate oxide field acceleration factor of 0.231 cm/MV are all extracted based on experimental data. The results in this work also provide a reference for reliable design by discussing the dependence of lifetime on stress, voltage and temperature. The main physical mechanism for recovery process of threshold voltage degradation after NBTI stress is confirmed to be the passivation of interface traps due to back diffusion of H_2.

References

[1] Ritzenthaler R, Schram T, Spessot A, Caillat C, Cho M, Simoen E, Aoulaiche M, Albert J, Chew S, Noh K B, Son Y, Mitard J, Mocuta A, Horiguchi N, Fazan P and Thean 2016 *IEEE Trans. Electron Dev.* **63** 265

[2] Neugroschel A, Bersuker G, Choi R and Lee B H 2008 *IEEE T. Dev. Mater. Rel.* **8** 47

[3] Mahapatra S, De S, Joshi K, Mukhopadhyay S, Pandey R K and Murali K V 2013 *IEEE Electron Dev. Lett.* **34** 963

[4] Yang H, Hwang W and Chuang C 2011 *IEEE T. VLSI. Syst.* **19** 1192

[5] Wahab Y A, Soin N, Shahabuddin S and Hussin H 2014 *IEEE International Conference on Semiconductor Electronics*, 27–29 August, 2014, Kuala Lumpur, Malaysia, p. 209

[6] Xu R R, Zhang Q Z, Zhou L D, Yang H, Gai T Y, Yin H X and Wang W W 2022 *Chin. Phys. B* **31** 017301

[7] Cao Y R, Yang Y, Cao C, He W L, Zheng X F, Ma X H and Hao Y 2015 *Chin. Phys. B* **24** 097304

[8] Tang H L, Xu B L, Zhuang Y Q, Zhang L and Li C 2016 *Acta Phys. Sin.* **65** 168502 (in Chinese)

[9] Zhang Y, Pu S, Lei X Y, Chen Q, Ma X H and Hao Y 2013 *Chin. Phys. B* **22** 117311

[10] Xu H, Yang H, Wang Y R, Wang W W, Luo W C, Qi L W, Li J F, Zhao C, Chen D P and Ye T C 2016 *Chin. Phys. B* **25** 087306

[11] Eghbalkhah B, Gharavi S A K, Afzali-Kusha A and Ghaznavi-Ghoushchi M B 2013 *International Conference on Design & Technology of Integrated Systems in Nanoscale Era*, 26–28 March, 2013, Abu Dhabi, United Arab Emirates, p. 151

[12] Schlunder C, Proebster F, Berthold J, Gustin W and Reisinger H 2015 *IEEE International Integrated Reliability Workshop*, 11–15 October, 2015, South Lake Tahoe, USA, p. 81

[13] Parihar N, Goel N, Chaudhary A and Mahapatra S 2016 *IEEE Trans. Electron Dev.* **63** 946

[14] Goel N, Joshi K, Mukhopadhyay S, Nanaware N and Mahapatra S 2014 *Microelectron. Rel.* **54** 491

[15] Mukhopadhyay S, Goel N and Mahapatra S 2016 *IEEE Trans. Electron Dev.* **63** 4038

[16] Joshi K, Mukhopadhyay S, Goel N, Nanware N and Mahapatra S 2014 *IEEE Trans. Electron Dev.* **61** 408

[17] Naphade T, Goel N, Nair P R and Mahapatra S 2013 *IEEE International Reliability Physics Symposium*, 14–18 April, 2013, Monterey, USA, p. XT.5.1

[18] Boo A A and Ang D S 2012 *IEEE Trans. Electron Dev.* **59** 3133

[19] Lee J and Oates A S 2010 *IEEE T. Device Mater. Rel.* **10** 174

[20] Hussin H, Muhamad M, Abdul Wahab Y, Shahabuddin S, Soin N and Bukhori M F 2013 *IEEE International Conference of Electron Devices and Solid-State Circuits*, 3–5 June, 2013, Hong Kong, China, p. 1

[21] Islam A E, Kumar E N, Das H, Purawat S, Maheta V, Aono H, Murakami E, Mahapatra S and Alam M A 2007 *IEEE International Electron Devices Meeting*, 10–12 December, 2007, Washington, USA, p. 805

[22] Mahapatra S (ed.) 2016 *Fundamentals of Bias Temperature Instability in MOS Transistors* (New Delhi: Springer), pp. 209–263

[23] Mahapatra S, Goel N, Desai S, Gupta S, Jose B, Mukhopadhyay S, Joshi K, Jain A, Islam A E and Alam M A 2013 *IEEE Trans. Electron Dev.* **60** 901

[24] Krishnan AT, Chancellor C, Chakravarthi S, Nicollian PE, Reddy V, Varghese A, Khamankar RB and Krishnan S 2005 *IEEE International Electron Devices Meeting Technical Digest*, 5 December, 2005, Tempe, USA, p. 688

[25] Mahapatra S, Islam A E, Deora S, Maheta V D, Joshi K, Jain A and Alam M A 2011 *IEEE International Reliability Physics Symposium*, 10–14 April, 2011, Monterey, USA, p. 6A.3.1

[26] Alam M A 2003 *IEEE International Electron Devices Meeting*, 8–10 December, 2003, Washington, USA, p. 345

[27] Chakravarthi S, Krishnan A, Reddy V, Machala C F and Krishnan S 2004 *IEEE International Reliability Physics Symposium*, 25–29 April, 2004, Phoenix, USA, p. 273

[28] Maheta V D, Olsen C, Ahmed K and Mahapatra S 2008 *IEEE Trans. Electron Dev.* **55** 1630

[29] Schlunder C, Hoffmann M, Vollertsen R, Schindler G, Heinrigs W, Gustin W and Reisinger H 2008 *IEEE International Reliability Physics Symposium*, 27–30 April, 2008, Phoenix, USA, p. 79

[30] Duhan P, Rao V R and Mohapatra N R 2017 *IEEE Trans. Electron Dev.* **64** 4018

[31] Guo Z C 2015 *Timing Degradation Analysis of Radiation Combined Effect on Space Digital Circuit*, MS Dissertation (Xian: Xidian University) (in Chinese)

[32] Zeng Y, Li X J, Wang Y L, Sun Y B, Shi Y L, Guo A, Hu S J, Chen S M and Zhao Y H 2017 *Microelectron. Rel.* **75** 20

[33] Kumar S V, Kim C H and Sapatnekar S S 2009 *IEEE Trans. Dev. Mater. Rel.* **9** 537